Pure & Appl. Chem., Vol. 56, No. 2, pp. 215-230, 1984.
Printed in Great Britain.

0033-4545/84 $3.00+0.00
Pergamon Press Ltd.
©1984 IUPAC

BASIC PHENOMENA IN REACTIVE LOW PRESSURE PLASMAS USED FOR DEPOSITION AND ETCHING – CURRENT STATUS

Guy Turban

Laboratoire de Physique Corpusculaire, E.R.A. 924
Université de Nantes, 2 Rue de la Houssinière, 44072 Nantes Cedex, France.

Abstract – Recent developments in the basic mechanisms of silane plasma deposition as well as in elementary processes of silicon and silicon dioxide dry etching by fluorinated plasmas are reviewed. The electron-impact reactions, gas phase ion-silane and radical-silane reactions are discussed. The tentatives at the modelling of plasma transport and deposition are also examined. The different dissociation pathways for CF_4, C_2F_6 and CF_3H are surveyed in the light of recent mass and optical spectrometric studies. Finally, the surface chemistry of the etching process and the kinetic analysis of the plasma reactor are outlined.

INTRODUCTION

The use of glow discharges in semiconductor applications has been developped in two very important directions in recent years.

Firstly, discharges have been used for the deposition of amorphous hydrogenated silicon by decomposition of monosilane (SiH_4) to give a - Si:H, which is an important electronic material extensively used for solar cells, thin film field-effect transistors (F.E.T.) and xerography. The silicon or the silicon-carbide films obtained by this technique contain 3-40 atom % hydrogen whose primary role is to neutralize the high density of defects in the band gap. This leads to a great improvement in electronic properties such as photoconductivity, susceptibility to doping, etc... Glow discharge preparation in films from mixtures of disilane (Si_2H_6), and/or silane with hydrocarbon gases, alkylsilanes and germane is also an active research area.

Secondly, the use of active species (atoms, radicals, ions), formed in halogenated glow discharge, have been used to selectively etch the various solid materials involved in V.L.S.I. circuit fabrication. Major advances have been obtained by this so-called "dry processing" in high resolution pattern delineation (~ 1 to 3 µm). The plasma etching of silicon and its compounds (SiO_2, Si_3N_4) constitutes the most important application. There are increasing studies concerned with other technologically important materials such as aluminum, GaAs, InP, silicides, and polymers. In order to obtain volatile products from the plasma-surface interactions, the halogenated gases (mainly CF_4, C_2F_6, CF_3H, SF_6, CCl_4, Cl_2) are used.

We have restricted this review to the two main fields in which the basic mechanisms are best known : deposition of a-Si:H film from silane plasmas, and etching of silicon and SiO_2 with fluorinated plasmas. Taking into consideration the abundant literature on these two subjects we have chosen to emphasize the recent results which shine some light on the plasma chemistry of these systems.

BASIC MECHANISMS OF SILANE PLASMA DEPOSITION

Electron impact action on silane

In the recent years, a better understanding of the electron-silane collision processes has been obtained. Table 1 gives the dissociation enthalpies calculated from bond strengths and heats of formation.

The smallest amount of energy required to dissociate silane (2.16 eV) corresponds to the threshold of the dissociative electron attachment. According to the estimation of Haller (2) the dissociative attachment cross-section for silane is 6×10^{-19} cm². Four reactions account for this cross-section : the formation of SiH_2^- and SiH_3^- (3) and two dissociative detachments following the SiH_4^- appearance (2):

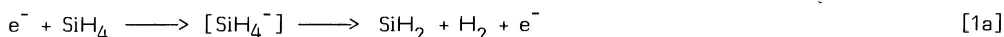

$$e^- + SiH_4 \longrightarrow [SiH_4^-] \longrightarrow SiH_2 + H_2 + e^- \quad [1a]$$

$$\longrightarrow SiH_3 + H^- \quad [1b]$$

TABLE 1. Dissociation enthalpies of SiH_4 (from (1))

$e^- + SiH_4$ ——>	$SiH_3 + H + e^-$	H =	4.04 eV
	$SiH_2 + H_2 + e^-$		2.16
	$SiH_2 + 2H + e^-$		6.7
	$SiH + H + H_2 + e^-$		5.7
	$Si + 2 H_2 + e^-$		4.2
	$Si + H_2 + 2H + e^-$		8.7
	$Si + 4H + e^-$		13.2

The electron impact dissociation following molecular electronic excitation is one of the main dissociation pathways of molecules (4). But most of the resulting products are unexcited species (ground state free radicals) which makes them difficult to detect. Following Winters' method (5) based on a surface technique, Perrin et al. (6) have recently measured the dissociation cross-section of SiH_4 and Si_2H_6. According to an U.V. absorption study of silane (7) it has been assumed that the threshold for electron impact excitation of silane is close to that for the U.V. absorption (i.e. 7.8 eV) (1) (8). Perrin et al. also agree with this assumption. Starting from the same considerations, Haller (2) quotes 7.48 eV as the best estimate for this threshold. The maximum of the dissociation cross-section for silane as measured by Perrin et al. and estimated by Haller are reported in the table 2.

TABLE 2. Maximum value of silane dissociation cross-section

After Perrin et al (6)	12×10^{-16} cm² at 60 eV
After Haller (2)	24.6×10^{-16} cm² for $\varepsilon > 22.4$ eV

Another dissociation cross-section has recently been derived by De Joseph et al. (9) from experimental measurements in a silane d.c. discharge.

The measurements of the dissociative ionization cross-section were done with a quadrupole mass spectrometer and based upon a comparison with ethylene (1) (8). The published values are compared in the table 3.

TABLE 3. Values of silane dissociative cross-section at 50 eV

Lampe (cited in 6)	Perrin (6)	Turban (1)
6×10^{-16} cm²	$5.0 \pm 0.9 \times 10^{-16}$ cm²	2.1×10^{-16} cm²

With an electron energy above 50 eV the ionization and the dissociation into neutral fragments have an equal probability (6).

Only a few percent of the neutral fragments are produced in excited states. As a consequence the main channels for the silane dissociation processes are difficult to establish. Turban et al. (11) assume a probability of 70 % for the SiH_2 production near threshold, by analogy with the dissociative ionization process. Following the same line of argument (ion core model) Perrin et al. (6) estimate dissociation probabilities up to 46 % for SiH_2 production at 60 eV, and 36 % for SiH_3.

Silane photolysis dissociation proceeds by pathways which may be different from those of electron impact since, for the latter, electrons will not only induce optically allowed transitions but also optically forbidden transitions. However the results of Perkins et al. (12) on silane photolysis with 8.4 eV photons give dissociation probabilities of 83 % (SiH_2) and 17 % (SiH_3) which suggests trends analogous to the above speculations on electron impact dissociation channels, i.e. a predominance for SiH_2 generation.

The emission cross-sections of various electronically excited fragments (i.e. SiH*, Si*, H*, etc...) from SiH_4 and Si_2H_6 have recently been published by Perrin et al. (13) (14). In the case of silane, all neutral excited states come from dissociation processes involving excited or superexcited states (neutral states lying above the first ionization potential).

Reactions in silane glow discharges

Electron impact decomposition. The kinetic study of the silane glow discharge decomposition has been undertaken by several authors using mass spectrometry (1) (8) (15)-(17), infrared absorption spectroscopy (9) and optical emission spectroscopy (18). The first problem encountered is to establish and define the correlation which exists between the electronic parameters of the plasma (electron energy, electron density) and the degree of decomposition of silane. Most of the studies were conducted with silane diluted in noble gases in order to minimize secondary reactions between reactive fragments (see below). In a tubular plug flow reactor and with a d.c. discharge, Nolet (16) determined a first-order rate constant for silane decomposition, a constant which is proportional to the electron density and dependent on the electron temperature.

Turban et al. (15) measured the mean electron density $< n_e >$ in a 5 % silane — 95 % helium r.f. discharge by microwave interferometry and found it to be proportional to the square root of the r.f. power. Considering the plasma as a complete backmix reactor they obtained a gas flow balance equation which gives an adequate description of the decomposition of silane as measured by mass spectrometry (1) (8). A fit of the calculated silane concentration to their experimental measurements enabled them to deduce a rate constant k_1 (sec^{-1}) for the silane dissociation. This constant obeys a square root law as a function of the r.f. power as did $< n_e >$. Thus these results indicate that the electron density controls the dissociation according to the rate constant $k_1 = k_d < n_e >$ with $k_d = < \sigma_d v_e >$ where σ_d is the dissociation cross-section and v_e the electron velocity.

De Joseph et al. (9) measured the silane decomposition in a d.c. discharge by infrared adsorption for a 1 % SiH_4 99 % Argon, Helium or Nitrogen mixture. In the case of helium and argon and with low discharge current, the results agree with a first-order decomposition. In the SiH_4-N_2 mixture the results show a different behavior, probably due to a contribution of N_2*or N(4s) to silane decomposition, as suggested by the reaction of active nitrogen with silane (19).

Hydrogen abstraction. Mass spectrometric measurements in silane plasmas proved that H_2 is an important product of decomposition (20) (21). The optical emission spectrum of silane glow discharges reveals the presence of atomic hydrogen (22) — (26) which is a primary product of the electron impact dissociation of silane (cf. Table 1) and/or the result of H_2 dissociation. The abstraction reaction :

$$H + SiH_4 \longrightarrow SiH_3 + H_2 \qquad [2]$$

is also known to have a substantialrate constant : 0.43 x 10^{-12} to 8.5 x 10^{-12} cm^3/sec per various authors (cf references in (1)). It was found that the addition of H_2 to a SiH_4-He discharge increases the Si_2H_6 concentration by a factor 5 (1) (11). Since the most probable mechanism for Si_2H_6 formation is the following sequence :

$$2\,SiH_3 \longrightarrow SiH_2 + SiH_4 \qquad [3a]$$

$$SiH_2 + SiH_4 \longrightarrow Si_2H_6 \qquad [3b]$$

The enhancement of Si_2H_6 production rate in a silane plasma with H_2 addition may be interpreted as a result of the increase in the SiH_3 production through the abstraction reaction [2]. Owing to the presence of H_2 and H in all silane plasmas, it is obvious that this reaction brings another route for the silane decomposition. Similarly the insertion [3b] is also a source of consumption of silane, depending on the SiH_2 concentration.

Ion-molecule reactions. Turban et al. (20) (21) have shown the predominance of the SiH_3^+ ion over the SiH_2^+ ion in silane glow discharges and explained it by ion-molecule mechanisms such as (27) (28) :

$$SiH_2^+ + SiH_4 \longrightarrow SiH_3^+ + SiH_3 \qquad [4]$$

The influence of the reactor parameters (silane partial pressure, flow rate, power) on the relative abundance of the various SiH_n^+ ions have been studied. The experimental trends are well understood in solving the balance equations for the ion densities (1) (8). Other authors obtained similar results (29)-(32). In $SiH_4 - CH_4$ and $SiH_4 - C_2H_4$ plasmas (33) (34) the ionic spectrum is also dominated by ion-molecule reactions such as :

$$SiH_2^+ + CH_4 \longrightarrow SiCH_4^+ + H_2 \qquad [5]$$

Two other types of reactions are concerned with modifying the population of SiH_n^+ ions relative to that issued from electron impact (8) :

(i) the ionisation of SiH_n radicals

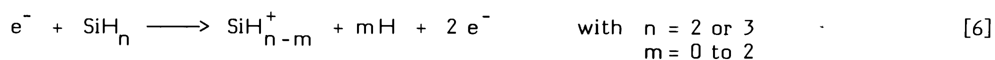

$$e^- + SiH_n \longrightarrow SiH_{n-m}^+ + mH + 2e^- \quad \text{with } n = 2 \text{ or } 3,\; m = 0 \text{ to } 2 \qquad [6]$$

(ii) the ion-molecule reactions involving H_n^+

$$H_n^+ + SiH_4 \longrightarrow SiH_3^+ + H_2 + H_{n-1} \qquad [7]$$

With the aid of isotopic labelling technique, it has been shown that the presence of H_2^+ and H_3^+ in the silane discharge gives rise to a supplemental increase of SiH_3^+.

The ionic abundance of $Si_2H_n^+$ ions varies also with pressure, flow rate and power. Some of them (for example ~ 40 % in $SiH_4 - He$ discharge (8)) come from direct electron impact ionization of the Si_2H_6 synthetized in the plasma. Another part originates from ion-molecules reactions such as :

$$SiH_2^+ + SiH_4 \longrightarrow Si_2H_n^+ + \text{etc...} \qquad n = 2 \text{ to } 5 \qquad [8]$$

In pure silane discharges several authors (29) - (32) observed the formation of $Si_nH_m^+$ clusters bearing up to 9 silicon atoms. Drevillon et al. (35) reported the existence of negative ion clusters bearing up to 6 silicon atoms.

The rate constants for the ion-molecule reactions [4] [8] are in the range of 2 to 4 x 10^{-10} $cm^3 sec^{-1}$. Haller (2) has recently pointed out that such reactions rates exceed by about 50 times the electron impact fragmentation rate if we suppose a mean electron energy of 1.46 eV. His calculation confirms that, with a mean electron energy of 4-5 eV as assumed in a $SiH_4 - He$ plasma at 150mtorr, the electron impact must be the main source of the consumption of SiH_4 (15). Therefore the determination of the electron energy distribution is crucial. With the Langmuir probes method Kocian et al. (36) obtained an electron temperature varying from 1 eV up to 3 eV in silane and silane-argon discharges at 500 mtorr. Bourquard et al. (37) pointed out the non-Maxwellian nature of the electron energy distribution. Optical measurements gave electron temperature values ranging from 1.6 up to 2.5 eV (38).

From these various results we can conclude that both electron impact fragmentation and ion-molecule reactions are competitive routes for the silane consumption. The domination of either electron impact processes or ionic reactions depends on discharge conditions.

Radical-molecule reactions. Among the neutral molecular fragments (SiH_3, SiH_2, SiH and Si) resulting from the electron impact dissociation of silane, only Si and SiH have been detected by emission spectroscopy (22) – (26), (18), and Si atoms by absorption spectroscopy (164). Attempts to detect electronic emission from SiH_2 or SiH_3 excited states in glow discharges have failed until now (39). Recently the emission from SiH_2^* has been observed in the decomposed gas produced by the infrared multiphoton dissociation of silane (10). The very sophisticated technique called C.A.R.S. (Coherent anti-Stokes Raman spectroscopy) has been recently used in order to detect non-emissive neutral species in a silane plasma (40). Schmitt et al. (165) used laser fluorescence to detect the SiH ground-state radical. Kampas and Griffith (23) (24) showed that Si* and SiH* are primary products of electron impact dissociation of excited silane molecules. The relative intensities of these lines have been studied as a function of deposition conditions (24) – (26).

Until now it has not been possible to determine anything about the production and the reaction of SiH_2 and SiH_3 in silane glow discharges by means of optical emission spectroscopy. However abundance of literature exists on SiH_n radical reactions studied by photolytic methods (cf. references cited in (1)). Owing to these studies, radical reactions are suspected to have an important role in the silane discharge (41). The use of isotopic labelling coupled with mass spectrometry has proved to be an invaluable method for obtaining some insights into these radical reactions (11) (33).

Turban et al. (1) (8) have detected from 14 up to 27 % of partially deuterated silanes in a $SiH_4 - SiD_4$ discharge. Two reactions were invoked as an explanation of these results :

(i) the disproportionation reaction :

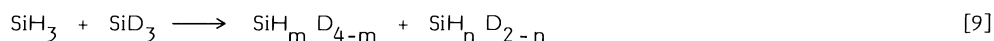

$$SiH_3 + SiD_3 \longrightarrow SiH_m D_{4-m} + SiH_n D_{2-n} \qquad [9]$$

(ii) the recombination reaction :

$$D + SiH_3 \longrightarrow SiH_3D \qquad [10]$$

In the same plasma conditions the synthetized disilane contains all the possible degrees of deuteration, implying the presence of third generation reactions, such as :

$$SiHD + SiH_2D_2 \longrightarrow Si_2H_3D_3 + \text{etc...} \qquad [11]$$

This study reveals an extraordinary interwoven chemistry when silane partial pressure is sufficiently high (50 mtorr for example).

The radical reaction chain leading to bond cleavage, rearrangement and polymerization is believed to bring an alternative route into silane activation. The dilution of silane in noble gases provides an interesting means for reducing these neutral reactions. For example it has been calculated (1) (8) that, during the diffusion of the SiH_2 radical from the gas phase to the walls of a 7.5 cm diameter

tubular reactor in a SiH_4 – He mixture, the volume losses due to radical insertion [3b] will be negligeable at 150 mtorr but will represent 40 % of all the volume and surface losses at 1 torr. By this mechanism Kampas (18) explains why the deposition rate of a-Si :H films does not decrease with the dilution of silane. The powder formation may be regarded as a consequence a gas-phase polymerization produced by radical reactions, although ionic condensation cannot be excluded. A comparison of the different typical rates for electron impact, radical and ionic reactions have been reported in a pure silane d c discharge (42).

Heterogeneous reactions in silane plasma.
A review of the numerous studies on the alteration of the properties and the structure of a-Si :H films according to the deposition conditions is beyond the scope of this paper. The reader may refer to the many excellent reviews on this subject e.g. (43) (44).

Modelling of plasma deposition. Some attempts have been published on the mathematical analysis of the mass transfer in the glow discharge deposition method based upon the assumption that neutral species are the main intermediates (45) (46). We report here the recent results published on the mechanism of plasma deposition from silane.

Street et al. (47) have studied the deposition rate of a-Si :H film as a function of the silane dilution and the r.f. power. At low power (~1 W) they observed a deposition rate independant of the SiH_4 concentration. As the power is raised, the rate depends on the dilution. Two regimes are distinguished : at low power the supply of silane is not the limiting process, but at high power and/or low silane concentration the deposition rate is limited by the silane depletion. These authors defined these regimes as the silane excess regime and the silane depletion regime. In correlation with these two regimes, they observe that the photoluminescence of the a-Si :H film is maximum for samples obtained with low power, a silane concentration $\gtrsim$10 % and a deposition temperature of 200-300°C.

The depletion regime of silicon deposition was studied by Turban et al. (1) (15) in a SiH_4-He mixture. In such a regime all the injected SiH_4 molecules are used to build up the silicon film (i.e. conversion of 100 %). A kinetic model has been developed in which neutral SiH_n (n = 2 or 3) free radicals are produced by electron impact excitation of SiH_4, and transported to the substrate by diffusion. Experimental conditions were chosen so that gas phase polymerization was limited. The sticking coefficients of SiH_n species on the growing film are supposed to be large (δ= 0.1 to 1). The surface reaction time was very short compared, with the diffusion time of species from gas to surface (1) (8) :

$$\Lambda^2 / D \; > \; 2R / \delta \bar{v} \qquad [12]$$

where Λ is the diffusion length (R/2.4), R the reactor tube radius and $\bar{v}$ the mean thermal velocity of SiH_n radicals. In this diffusion controlled regime, Turban et al. (15) calculated the diffusional flux ϕ_o of SiH_n radicals in a tubular reactor by using an experimental value of the silane decomposition rate k_1. The comparison with the deposition rate ϕ_e measured by weighing gives a ratio ϕ_e / ϕ_o = 1.14 to 0.82 depending on the radial concentration profile assumed in the ϕ_o calculation. These results bring forward evidence that SiH_n neutral free radicals are predominant for the silicon mass transport in these experimental conditions.

Catherine et al. (48) have measured in similar experimental situations, the ion flux reaching the substrate by using a small grid probe in a C_2H_4– SiH_4–He discharge. The ratio of ion flux ϕ_i to ϕ_e the flux of condensed particles is found to be 0.16 to 0.2, confirming the result of Turban concerning the predominance of the neutral deposition. In the so-called d.c. proximity arrangement they measured a ratio ϕ_i / ϕ_e in the range 2 x 10^{-3} to 4 x 10^{-3}. The main contribution of the ion flux appears to be a structural change of the growing film, induced by the most energetic ions which represent only a minor part of ϕ_i. In a low pressure multipole plasma with 35 – 65 eV electrons Drevillon et al. (30) have found ratio ϕ_i / ϕ_e varying from 0.2 to 0.8 as the pressure is lowered from 2mtorr to 0.3 mtorr. A comparison of the films deposited from dominant ionic flux with those due to neutral deposition is made by these authors (49).
From the results of these different works one can conclude that two classes of active species contribute to film growth in silane plasmas depending upon discharge conditions : essentially neutral fragments in typical rf glow discharges and d.c.-proximity discharges, ionic species in more particular plasmas e.g. multipole plasmas. Depending on the silane dilution the active species can transport one or more silicon atoms as shown in the plasma analysis. In any case the silane plasma deposition method does not represent a "pure" deposition in the sense that both species are always present, even if only as a minor proportion. Such a situation differs from the homo-C.V.D. process in which SiH_2 radical is believed to be the unique intermediate in transport of silicon to the growing film (50).

Hydrogen heterogeneous reactions. If SiH_2 is the key precursor of the a-Si :H deposition from silane glow discharge, as proposed both by film chemistry arguments (51) and silane dissociation considerations (15) (20), heterogeneous dehydrogenation must be considered to account for the large decrease in H content (5 - 40 atomic % in major films). Two reactions have been proposed (8) (24) (41) (52) :

(i) an heterogeneous disproportionation reaction :

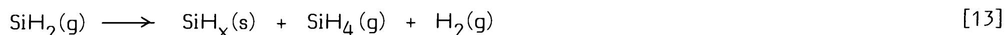

$$SiH_2(g) \longrightarrow SiH_x(s) + SiH_4(g) + H_2(g) \qquad [13]$$

(ii) a dehydrogenation reaction, induced by ion bombardment

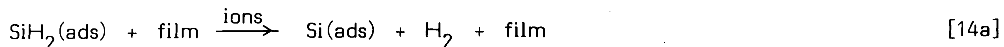

$$SiH_2(ads) + film \xrightarrow{ions} Si(ads) + H_2 + film \quad [14a]$$

$$Si(ads) + H + film \quad [14b]$$

Complementary with these reactions involving SiH_2, atomic hydrogen reactions can explain hydrogen addition and dangling bond passivation by analogy with gas phase reactions (53). Infrared absorption studies of film deposited from a $SiH_4 - He - D_2$ plasma and simultaneous mass spectrometric control of gaseous phase (8) (11), bring forth evidence of a direct incorporation of D atoms and/or ions in the growing film.

When a D_2 plasma interacts with a-Si:H film, the formation of SiD_4 and Si_2D_6 is detected by mass spectrometry (1) (11) (17) (20). This formation is believed to be the result of an etching of the film by hydrogen atoms from the gas phase. The interaction of a hydrogen d.c. discharge with silicon has been studied by Webb and Veprek (54) (55). With an intense discharge (high current density) and low temperature substrate (water cooling),a plasma assisted transport is observed. An erosion rate of the silicon is accompanied by a deposition rate of silicon in another part of the discharge tube where the conditions are : low current density and high temperature. Wagner and Veprek (17) observed the formation of gaseous silane in the plasma tube in agreement with the result obtained by Turban et al. (20). The fact that microcrystalline films are deposited when the optical emission from H and H_2 is larger than the optical emission from SiH (56) suggests that atomic hydrogen plays a role in the bond breaking of Si — Si bond. Wagner and Veprek have performed a mass spectrometric study of the silicon/hydrogen low-pressure system. At very low flow rate ("partial chemical equilibrium") when the residence time of molecules is $\gtrsim 5$ sec, the silane concentration is the same in either a silane discharge or in a Si/D_2 plasma. At high flow rate the two systems exhibit different silane concentrations. The former case favours microcrystalline silicon formation. These authors believe that the decisive parameter controlling the structural properties of the deposit is the departure of the system from this partial chemical equilibrium (56).

CHEMICAL PHYSICS OF FLUORINATED PLASMAS USED FOR SILICON AND SILICON DIOXIDE ETCHING

Since 1977 a considerable amount of literature has been published concerning the plasma etching of the materials used for integrated circuit fabrication. There are excellent reviews on industrial aspects (58) (59) as well as on the various basic conceptions with regards to dry processing (60) — (70). In this paper we intend to emphasize the basic mechanisms which can be drawn from the relevant publications. We shall examine with some details the situation in fluorinated plasmas interacting with silicon and silicon dioxide. For several other aspects which are of primary importance from an industrial point of view : aluminum etching in chlorine containing plasmas (69), etching of III-V compounds (71), silicides (72) and organic materials (65) and reactive ion beam etching (73), the reader may refer to appropriate literature.

Chemical physics of fluorinated plasmas

There is general agreement in the belief that atoms, radicals and charged particles (ions, electrons) are the main active species which confer their etching or deposition properties to discharges. We are going to detail the current situation in reaction mechanisms within the fluorinated plasmas. In table 4 are listed the main electron-molecule processes responsible for reactive species production in the case of CF_4, C_2F_6, CF_3H, SF_6 and CCl_4.

With a low electron energy ($\lesssim 5$ eV), even as low as thermal energy in specific cases, the dissociative electron attachment represents the first dissociation mechanism for halogenated gases. The attachment cross-sections appear to be rather low ($< 10^{-17}$ cm²) for the fluorocarbons (74)-(76), however the presence of a majority of low energy electrons in discharges may result in a significant dissociation rate through dissociative attachment. SF_6 and CCl_4 represent two examples for which the dissociative attachment process is probably the main decomposition source in etching plasmas. It must be remember that electron detachment :

$$e^- + F^- \longrightarrow F + 2e \quad [15]$$

is a rapid reaction. Hence the dissociative attachment processes are a fluorine (or chlorine) source for the discharge.

Winters et al. (78) proposed for the first time that the CF_4 dissociation in an r f discharge mainly proceeds via neutral fragmentation resulting from electronic excitation of the molecule. Winters and Inokuti (79) measured the dissociation cross-section for the fluoroalkanes such as CF_4, CF_3H, C_2F_6 and C_3F_8. The cross-section maximas are in the range of 5 to 10×10^{-16} cm² and the dissociation threshold at up to 12.5 eV (see Table 4).

TABLE 4. Major electron impact dissociation channels for some halogenated polyatomic molecules.

Reaction	Process	Threshold (eV)	Max. cross-section (cm^2)	Reference
$e^- + CF_4$	$CF_3 + F^-$	4.65	6×10^{-19}	(74) (77)
	$CF_3^- + F$	6.9	4×10^{-19}	id°
	$CF_3 + F + e^-$	12.5	5.55×10^{-16}	(79)
	$CF_3^+ + F + 2e^-$	15.4	4.68×10^{-16} at 70 eV	(155)
$e^- + C_2F_6$	$C_2F_5 + F^-$	2.1	5.10×10^{-18}	(74)
	$CF_3 + CF_3^-$	2.2	1×10^{-18}	
	$CF_2 + CF_4 + e^-$	12.5	8.6×10^{-16}	(79)
	$CF_3 + CF_3 + e^-$			
	$C_2F_5 + F + e^-$			
	$CF_3^+ + CF_3 + 2e^-$	15.4	7.79×10^{-16} at 70 eV	(155)
	$C_2F_5^+ + F + 2e^-$	16.05		
$e^- + CF_3H$	$CF_2H + F^-$	2.2		(77)
	$CF_2 + HF + e^-$	12.5	5.8×10^{-16}	(79)
	$CF_3 + H + e^-$			
	$CF_2H + F + e^-$			
	$CF_3^+ + H + 2e^-$	14.7	4.47×10^{-16}	(155) (156)
	$CF_2H^+ + F + 2e^-$	16.4		
	$CF_2^+ + H + F + 2e^-$	17.5		
$e^- + SF_6$	SF_6^-	0	5.2×10^{-14}	(157)
	$SF_5^- + F$	0	4×10^{-16}	(158)
	$SF_5 + F^-$	2.2	6×10^{-16}	(159)
	$SF_5 + F + e^-$			(114)
	$SF_5 + F + 2e^-$	15.9	5.65×10^{-16} at 70 eV	(160) (161)
	$SF_4^+ + F_2 + 2e^-$	18.9		
$e^- + CCl_4$	$CCl_3 + Cl^-$	0	$\sim 10^{-14}$	(75)
	$CCl_2 + Cl_2^-$			(162)
	$Cl + CCl_3^-$			
	$CCl_3 + Cl + e^-$			(69) (163)
	$CCl_2 + 2\,Cl + e^-$			
	$CCl_2 + Cl_2 + e^-$			
	$CCl_3^+ + Cl + 2e^-$	11.83		
	$CCl_2^+ + Cl_2 + 2e^-$	16.1		

For CF_4 an agreement exists suggesting the following decomposition process :

$$e^- + CF_4 \longrightarrow CF_3 + F + e^- \qquad [16]$$

Winters bases his argument on the ion core model : the dissociation fragments come from a Rydberg state of the molecule which tend to dissociate as the ion core since the Rydberg electron is non-bonding (79). Various neutral fragments may results from electron impact dissociation of other molecules (C_2F , CF_3H, etc...) Melliar-Smith and Mogab (60) suggested a simple analogy with dissociative

ionization. Recent results obtained by optical emission spectroscopy (80) – (82) suggest decomposition pathways based on experimental observations. We shall follow these pertinent works (81) (82).

In order to estimate the relative density of ground-state neutral radicals from the emission intensity of similar excited species, a technique called "actinometry has been developped (83) – (85). This technique essentially consist of adding to the reactive mixture an actinometric gas, such as Ar or N_2 at a low known concentration (~ 1 – 2 %). The ratio of the F* intensity (for example) to the Ar* intensity is shown to be proportional to the ground state F atom density. However specific conditions must be satisfied : (i) the reaction leading to the excited states mainly arises by direct electron impact from the ground level, (ii) the radiative decay is predominant compared with the collisional quenching. This technique proved to be a useful tool to obtain the trends of the relative densities of several unstable species : F, CF, CF_2 and CF_3 (81) (83).

Decomposition scheme for CF_4. Several studies agree with the following sequence (81), (86) – (90) :

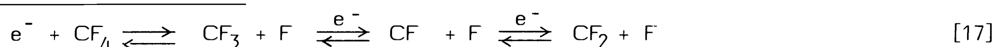

$$e^- + CF_4 \rightleftharpoons CF_3 + F \overset{e^-}{\rightleftharpoons} CF + F \overset{e^-}{\rightleftharpoons} CF_2 + F \qquad [17]$$

In a CF_4 r.f. plasma (0.5 torr, 50 W, 50 sccm), d'Agostino et al. (81) found the F, CF, CF_3 and CF_2 densities to be approximatively in the ratio 3: 4: 5: 6. The small proportion of CF_2 compared to CF_3 radicals was unexpected. Despite the fact that CF_3 is likely the first radical to be produced it may not be the most abundant. Thermochemical data reported in Table 5 indicate that it must be easier to break a F – CF_2 bond than F – CF_3 or F – CF bonds (90)

TABLE 5. Dissociation bond energies (eV) from thermochemical data for some fluorocarbon neutral species.

	Ref 90	Ref 77	Ref (87) (88)	Ref 153	Ref 154
D(F – CF_3)	5.6	5.62	5.69	5.39	5.26
D(F – CF_2)	2.2	3.8	3.83	4.74	4.15
D(F – CF)	6.1	5.36	5.35	5.13	4.66
D(C – F)	5.2			4.96	5.74
D(CF_2–CF_4)			2.39		
D(CF_3–CF_3)	4.4		4.17	3.04	4.20
D(F –C_2F_5)	5.5		4.96		
D(CF_2 –HF)			2.43		
D(H–CF_3)	4.6	4.61	4.52		
D(F –CF_2H)		5.47	4.91		

D'Agostino et al. (81) consider that the recombination reactions :

$$CF_{n-1} + F \longrightarrow CF_n \qquad [18]$$

are rapid for n = 1 to 3 but slow for n = 4.

Mass spectrometric measurements of CF_4 discharges(86) – (89),(63) bring forward evidence of C_2F_6 formation,but only traces of C_2F_4. Two reactions are supposed to be a trap for the CF_3 radical : the dimerization leading to C_2F_6 and the reformation of CF_4 (78) (89).

Decomposition scheme for C_2F_6. The mass spectrometric studies of a C_2F_6 rf plasma point out the formation of stable molecules : CF_4, C_2F_4 and C_3F_8 (87) (88). The CF_4 molar fraction can exceed that of C_2F_6 with a favorable choice of working parameters (low flow rates, rather high power). Optical measurements give the relative densities of F, CF, CF_3 and CF_2 ground species as follows : 1: 3: 3: 40 (81). Laser-induced fluorescence spectroscopy was used to detect ground-state CF_2 radicals in C_2F_6 and CF_4 plasmas (92). Measurements showed that CF_2 densities were significantly higher in the C_2F_6 plasma compared to CF_4 plasma, in agreement with the result of d'Agostino. The predominance of CF_2 and CF_4 can be explained in two ways :

— a rapid electron impact dissociation of CF_3 radical (as indicated in the CF_4 scheme),

— a direct decomposition of C_2F_6 into CF_2 and CF_4.

D'Agostino et al. (8) favor this last route already proposed by Flamm (105). The comparison of the various bond energies in C_2F_6 (Table 2) agrees with this process. A ratio of 0.3 has been found for atomic fluorine in a C_2F_6 plasma relative to a CF_4 plasma (81). A possible pathway is the decomposition of CF_n radicals or CF_4 molecules. A direct dissociation by the breaking of the $F - C_2F_5$ bond cannot be excluded. Such a reaction is plausible according to thermochemical data and ionic fragmentation. Finally the formation of C_3F_8 in the C_2F_6 discharge may arise from a reaction involving C_2F_5 : for example $C_2F_5 + CF_3 \longrightarrow C_3F_8$. The decomposition scheme for C_2F_6 would be, by decreasing order of importance :

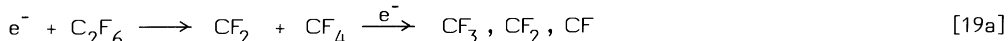

$$e^- + C_2F_6 \longrightarrow CF_2 + CF_4 \xrightarrow{e^-} CF_3, CF_2, CF \qquad [19a]$$

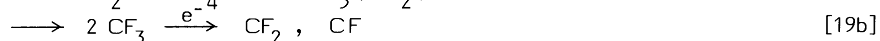

$$\longrightarrow 2\, CF_3 \xrightarrow{e^-} CF_2 , \; CF \qquad [19b]$$

$$\longrightarrow C_2F_5 + F \qquad [19c]$$

Decomposition scheme for CF_3H. The CF_3H decomposition mechanisms in a plasma have not been intensively studied. However Truesdale and Smolinsky (87) demonstrated the presence of CF_2 radicals by mass spectrometric measurements as well as in CF_4-H_2 plasma and C_2F_4 plasmas (93). H F was found to be the main decomposition product in the CF_3H discharge. These results are in favour of a decomposition into CF_2 and HF. However the formation of other stable molecules such as CF_4, C_2F_6 and mixed products (C_2HF, etc...) (87) (94) do not permit the exclusion of other dissociation pathways, even if of minor importance. The actinometric measurements obtained with a CF_4-H_2 discharge show that the density of CF_2 radicals is strongly increased compared with that in CF_4 plasma (X 4) (82). According to these results the decomposition scheme for CF_3H would be in decreasing order of importance :

$$e^- + CF_3H \longrightarrow CF_2 + HF + e^- \qquad [20a]$$

$$\longrightarrow CF_3 + H + e^- \qquad [20b]$$

$$\longrightarrow CF_2H + F + e^- \qquad [20c]$$

The second route was the only one postulated by Kushner (90). The last pathway, although thermodynamically unfavourable, is not unrealistic as regards to the ionic fragmentation.

In these different schemes only the radical reactions have been taken in account. This situation is believed to be suitable for the plasma etching mode (pressure about 0.1 to 1 torr). In the reactive ion etching mode (typically ~ 10 mtorr) the electron density is one order of magnitude greater ($\gtrsim 10^{10}$ cm^{-3} instead of $\sim 10^9$ cm^{-3}) and the electron energy is increased (90) (95) (96). Even if the neutral radical density still remains larger than the ion density (70), the chemical identity of the molecular ions will become more important than in the so called "plasma mode" (see below for the role of ions). Ion-molecule reactions with fluorocarbons are known and will distort the primary ion spectrum in some cases (97)—(99).

Hydrogen addition and film deposition. The introduction of hydrogen into a CF_4 plasma — or the use of CF_3H gas — is now a well-established method for etching SiO_2 more rapidly than Si (100) — (102). In situ Auger electron spectroscopy of Si and SiO_2 surfaces after etching in CF_2-H_2 glow discharges has shown that the selectivity max be explained by the role of carbon deposits on silicon surfaces (103). This film, not found on SiO_2 surfaces is presumed to be formed by CF_x radicals. Coburn and Kay (104) proposed the simplified concept of F/C ratio. Depending on this ratio of the reactive species in the fluorocarbon plasma, etching or polymerization is produced on the reactor walls. The hydrogen added to fluorocarbon gases tends to decrease the F/C ratio by consuming atomic fluorine. The mass spectrometric measurement of the $CF_4 - H_2$, CF_3H and the $C_2F_6 - H_2$ discharges (87) show a large concentration of HF. Optical spectroscopy of these discharges (82) confirmed these results and proved the validity of the F/C ratio concept. The general effect of introducing H_2 is to produce a spectacular increase in the CF and CF_2 density and to destroy F atoms (80) (70). The formation of a CH_xF_y polymer film (x = 0.03 to 0.34 and y = 0.73 to 1.55, depending on gases (88)) is observed on walls at ground or floating potential. Dilks and Kay (106) have noted the presence of $(CF_2)_n$ species in the effluents of fluorocarbon plasmas and have proposed that these are the precursors of the deposition. In a C_2F_4 plasma Millard and Kay (107) found a linear relationship between the CF_2^* intensity in the discharge and the polymerization rate of fluorocarbon film. In order to explain the final stoichiometry of the CF_x film deposited in a C_2F_4 discharge a fluorine elimination by an interaction of photons, ions and metastables is postulated (63).

D'Agostino et al. (82) developped a polymerization model based on optical measurements in which the the deposition rate is expressed by :

$$r_p \;\alpha\; R_g \cdot f(n_e) \qquad [21]$$

where R_g is the gas phase radical concentration and $f(n_e)$ the electron excitation function taken as representative of the charged particles responsible for surface site creation. In this work the CF and CF_2 radicals are considered to be precursors of deposition, with the main contribution being from CF.

A discrepancy in the role of ions proposed among the different authors: either activating the surface for polymerization (82) or preventing deposition, according to other authors (61). A general scheme for film formation was proposed by Flamm (108) based on the concept of unsaturated species (for example CF_2).

The oxygen addition. In industrial dry processing $CF_4 - O_2$ is certainly the most popular mixture used for polysilicon etching. When the oxygen is added to the CF_4 gas, the etch rate of Si has been found to increase substantially (about one order of magnitude)(110). Gas phase titration (109) and optical measurements (83) (80) (70) have shown an increase of the fluorine atom concentration with oxygen addition. On the contrary, a decrease of the electron density was found almost proportional to the oxygen addition and without any appreciable change in the energy distribution of these electrons (80). Sanders et al. (111) proposed the use of CO_2 as a substitute for O_2 and obtained a similar enhancement of the silicon etch rate. When CO_2 or CO are injected in a CF_4 discharge they cause a decrease of the discharge excitation efficiency, perhaps due to "cooling of" of the electron energy distribution (83).
Mass spectrometric analysis of the $CF_4 - O_2$ plasma gave the following products : CO, CO_2, COF_2, F_2 and F (86) (112). The chemistry accounting for the rate enhancement of F atoms and the synthesis of stable products is as yet uncertain. Recent kinetic measurements for reactions of CF_3 with O (^3P) in discharge flow experiments (113) gave a rate coefficient of $(3.1 \pm 0.8) \times 10^{-11}$ cm³/sec for the reaction written below :

$$CF_3 + O \longrightarrow CF_2O + F \qquad \text{at } 295 \text{ K} \qquad [22]$$

It was found that in the reaction between O_2 and CF_3 (2.2×10^{-13} to 1.24×10^{-12} cm³/sec) CF_2O represents less than 1 % of the final products, the main product is then supposed to be CF_2O_2. Therefore reaction [22] would be an important source of atoms in $CF_4 - O_2$ discharges as previously proposed (111) (112). With oxygen addition to CF_4 the consumption of CF_2 and CF radicals was detected by the actinometric method (80). Flamm et al. (70) believe that O and O_2 compete with atomic fluorine to remove CF_2 and produce COF_2, CO and CO_2.

It has been pointed out that in O_2-CF_4 and O_2-SF_6 discharges the silicon etch rate is proportional to the F atom concentration for only small amounts of oxygen (62) (109) (114). Nevertheless the direct correlation between the fluorine atom density and the silicon gasification rate is well established (115). The discrepancy observed in $CF_4 - O_2$ plasmas is attributed to the competitive absorption of F and O atoms on the silicon surface. In a recent optical study Kawata et al. (146) confirm this competitive model. There is a general trend in reactive plasma interaction with surfaces that all active species produced in the gas phase compete in surface reactions. For example dry etching of the polyimide Kapton in a $SF_6 - O_2$ plasma is produced both by F atoms and O atoms (116). Etching of Mo or W in F – rich plasmas is probably enhanced by an oxygen reaction with the surface (117).

Surface chemistry in plasma etching.

Isotropic etching of silicon. When silicon etching is produced only by atomic fluorine interaction, a circular (isotropic) profile with a radius equal to the etched depth is formed. The silicon etching rate has been measured in an F_2 flowing afterglow source, which provides F atoms with a Maxwell-Boltzmann kinetic energy distribution of average energy 0.04 eV and randomly directed towards the surface (115). In the range of an F density $n_F = 1 \times 10^{15}$ at/cm³ to $n_F = 5.1 \times 10^{15}$ at/cm³ the rate is expressed by :

$$R_{F(Si)} = (2.91 \pm 0.20) \times 10^{-12}\ T^{1/2}\ n_F\ \exp(-0.108\ \text{eV}/kT)\ \text{Å/min} \qquad [23]$$

where T is the substrate temperature (K), and k the Boltzmann's constant.

The reaction probability $\varepsilon_{F(Si)}$ defined as the ratio of the etchanf F atom flux to the incident F atom flux deduced from above experiment is given by :

$$\varepsilon_{F(Si)} = 0.116\ \exp(-E_a/kT) \qquad [24]$$

For a substrate temperature of 100°C Flamm et al.(115) found $\varepsilon_{F(Si)} = 0.004$ while Vasile and Stevie (118) obtained 0.016 with a beam of fluorine atoms produced by thermal dissociation of F_2 at 800°C and having a narrow distribution of kinetic energy centered at 0.19 eV. The free fluorine atoms react spontaneously with silicon surfaces to form the stable product SiF_4. But some other unstable products were also found, mainly SiF_2 (118) – (120). The chemiluminescence observed in plasma and afterglow experiments is assigned to the deexcitation of SiF_3^* formed by the reaction of SiF_2 with F or F_2 (119) (121). The reaction products of F atom with Si have been identified by mass spectrometry (118) : the lower limit of the ratio n_{SiF_2}/n_{SiF_4} was found to lie between 0.1 and 0.3.

An isotropic spontaneous etching of silicon can be obtained, without plasma, by the $XeF_2 - Si$ interaction (122) – (125). Etch products are SiF_4 for more than 85%, the rest of the products are composed of SiF, SiF_2 and possibly SiF_3. However the similarity between F/Si and XeF_2/Si interaction was recently questioned (126) (127) : in particular, with an equivalent pressure it has been shown that XeF_2 etches Si more than 10 times faster than do F atoms at room temperature. The very high reactivity of XeF_2 with silicon is attributed to a higher surface physisorption coming from the polarisability of XeF_2 (126).

Anisotropic etching of silicon. The importance of ion bombardment effects in plasma etching is clearly illustrated by the enhancement of the silicon etch rate when the substrate is negatively biased (63). If some of the substrate is masked with a photoresist, an anisotropic profile will result from the difference between lateral etching (i.e. spontaneous) and vertical etching. A set of basic experiments conducted with a neutral beam of XeF_2 or F_2 and ion beams of He^+, Ar^+ and Ne^+ permit Winters et al. to establish the main laws of ion-induced etching, sometimes called chemical sputtering (122)-(129). The reader is referred to a detailed discussion of this mechanism (64) (68) (125).
In the plasma etching context, Bruce (67) has recently reviewed the different means by which anisotropy is produced. The control of profile is essential in the integrated-circuit fabrication in order to obtain submicron dimensions. Two mechanisms have been proposed to explain the experimental results, both related to ion bombardment effects:

(i) the enhancement of etching rate by a clearing mechanism (68) (125). The ion bombardment clears the fluorinated layer formed on silicon as detected by X.P.S. measurements (130) by volatilization of SiF_4 possibly formed through a disproportionation reaction between two SiF_2 adsorbed species. The clean silicon surface is supposed to have a reaction coefficient higher than the fluorinated surface. From this point of view the role of ion bombardment would be to maintain a silicon surface clean of fluorine atoms.

(ii) the damage mechanism (65) (66) (70). Impinging ions produce lattice damage creating active sites (dangling bonds). Reaction of atomic fluorine with broken bonds is supposed to be higher than with the relativity stable SiF_2 surface.

In specific cases (CF_3Cl or $C_2F_6 - Cl_2$ plasmas) adsorbed "recombinant" species (CF_2, CF_3, C_2F_5) can induce films on sidewalls which destroy etchant species (atoms) by recombination. These radicals act as a passive etching barrier. On the bottom surface ion bombardment can stimulate desorption of the radicals and permit the etching reaction (131).

Etching of silicon dioxide. (1) by fluorine atoms. The kinetics of isotropic etching of SiO_2 by fluorine atoms has been studied with a flowing afterglow source (132). Without ion bombardment, F atoms react slowly with SiO_2 :

$$R_{F(SiO_2)} = (6.14 \pm 0.49) \times 10^{-13}\, n_F\, T^{1/2} \exp(-0{,}163\ eV/kT)\ \text{Å/min} \qquad [24]$$

In a $CF_4 - O_2$ discharge, excited with 13.56 MHz generator, Mogab et al. (109) obtained a rough proportionality between the F density and the SiO_2 etch rate (from 100 up to 300 Å/min). Under ion bombardment (100 kHz) the SiO_2 etching in F source plasmas was found proportional to ion flux (<2 mA/cm²) (70).
(2) by CF_n radicals. The use of plasmas with a high C/F ratio is required to selectively etch SiO_2 with respect to Si. The high concentration of CF_2 and CF radicals in such discharges indicates they are the probable etchant species of SiO_2. When adsorbed on SiO_2 surfaces, these unsaturated radicals can form carbon containing films that persist during etching. The ion bombardment effect could be due to a breaking of bonds in the oxide thus producing the anisotropic etching effect generally observed. It seems that CF_n radicals alone cannot etch SiO_2 "spontaneously" because they form a polymer film, thus the SiO_2 etching reaction requires a clearing or a damage mechanism (70). However Kushner (90) attributes the SiO_2 etching to all CF_n and F species (radicals and ions) without a specific role for ion bombardment.

Loading effect in a general sense. In many plasma etching systems the etch rate decreases as the area of material to be etched is increased. Mogab (134) showed that this effect was due to the depletion of the reactive species in the gas phase induced by an increased consumption at the surfaces. This so-called "loading effect" will exist in all systems for which the etch rate is limited by the concentration of active species. However electrode or wall materials containing oxygen (such as SiO_2, Al_2O_3) can be consumed during the etching process and the action of the liberated oxygen compensates the loading effect.

We would like to emphasize a general aspect of this loading effect for plasma chemistry. All modification of an heterogeneous reaction rate will in return produce cumulative modifications in other reaction rates,in the volume and on surfaces. Consequently the concentration of all stable molecules (and obviously unstable species) will be affected. Smolinsky and Flamm (86) pointed out, all other conditions being equal, that the introduction of a silicon sample in a CF_4 plasma modifies the molar fraction of C_2F_6 , a secondary product. A correlation was found between the SiF_4 concentration and the C_2F_6 concentration (89). The concentration of CF_4 , the injected gas, is dependent on the silicon surface to be etched. Turban et al. (135) interpreted this result as an indication of a second source of CF_4 , for example the reformation reaction $F + CF_3$.

The consumption of unstable species (F, CF_2) during etching has been shown by mass spectrometry and optical detection (88) (70) (146). The step by step effect of active species consumption upon the various reaction rates is complex to analyse. However it can be used as tool to gain some insight into the plasma reactions. For example when we use a $SF_6 - O_2$ plasma, known to be an F and O atom source, for etching silicon or polyimide (116), the concentration of SO_2, SOF_4 , SOF_2 and SO_2F_2 varies. F consumption during silicon etching induces an increase of all these secondary products, contrary to F and O consumption during polyimide etching. This comparison leads to the establishment of pathways for the secondary products formation which consume F or O species.

Plasma reactors

Apparatus considerations. (1) Physical variables. One of the major difficulties encountered by users of plasma etching apparatus is the very high number of parameters associated with the process. The previous paragraphs have shown the complexity of the heterogeneous and homogeneous chemical reactions. We are going to examine, in the last part, the main reactor parameters and how they act on the reaction rates. The interdependance of the macroscopic variables with the microscopic properties of the etching plasmas were emphasized by Kay et al. (63).

(i) the excitation frequency. Many plasma etchers are excited with 13.56 MHz frequency. But some industrial machines use low frequencies (50 – 400 kHz). Melliar-Smith and Mogab (60) believe that high frequencies are more efficient in producing the reactive species. By the aid of a simple model of the discharge Taillet (135) demonstrated that the energy of ions impinging the electrode would increase as the frequency decreases. An analysis of the ion behaviour as a function of the excitation frequency has been proposed by Bruce (136). In an Ar – Kr discharge at 0.3 torr the maximum energy of the ions reaching the electrode increase as frequency decreases, if we assume constant operating voltage, from 13 MHz to 15 kHz. The energy analysis of the ions at the electrode of a Cl_2 discharge demonstrated that both Cl^+ and Cl_2^+ ion distributions are higher in energy and magnitude at 100 kHz compared with 13 MHz.

(ii) the total pressure. In a sense frequency and pressure can be regarded as two interchangeable variables. Low pressure discharges produce higher voltage than those at higher pressure. The ion density in the plasma increases as the pressure decreases for the same power level (95). The so-called "reactive ion etching" or "reactive sputter etching" brings an enhancement of ion bombardment compared with the "plasma mode" and more anisotropic etching will result. Another pressure effect concerns the relative importance of volume reactions relative to surface reactions. The diffusion time of reactive species and the homogeneous reaction time are both pressure dependent (1). Low pressure enhances diffusion and limits volume reactions. We can expect a better homogeneity of the intermediate species in the gas phase. If the reaction is surface limited as supposed in plasma etching, the low pressure climinishes concentration gradients (

(iii) the flow rate. Five variables are influenced by flow rate : the pressure p, the input flow rate Q_M (torr.liter/sec), the pumping speed C(l/sec), the reactor volume V and the residence time t_R. The mean residence time $t_R = p\,V/Q_M$ spent by the molecules in the reactor gives the interrelation between these parameters (63). With varying the reactor pressure, two outcomes are available: at constant input flow rate t_R will vary; or to maintain t_R constant flow rate must be proportionately adjusted. For the same pressure and power various measurements indicate that the plasma will present different and sometimes contradictory properties depending on the flow rate value(63), (86)-(89), (137)-(139). Because of depletion phenomena, for long residence time the molecular nature of input gas is of little importance relative to its atomic stoichiometry. The residence time allows a kinetic analysis by using a plug flow model.

(iv) the substrate temperature. Etch rates usually follow an Arrhenius type law with substrate temperature :

$$R \;\alpha\; \exp(-E_a/kT) \qquad [25]$$

with an activation energy E_a depending on the material. In the case of a low volatility of the etchant products ($AlCl_3$, $InCl_3$) the substrate temperature will limit the etching process (140).

(v) the reactor geometry. Residence time and diffusion time depend on the geometrical dimensions of the reactor. The ratio of the powered electrode area A_t to that of the grounded electrode A_w is known to control the self-bias voltage in the r.f. discharge (141) (139). Very small electrode gaps (~ 6 mm for example), as used in some plasma etchers, achieve both very high etching rates and anisotropy.

(vi) application of superimposed voltage. The application of a d.c. voltage to the r.f. electrode produces an increase in the ion bombardment of the grounded electrode, resulting from an increase of the plasma potential (141) (143) (144). An alternative method consists in using the so-called "flexible diode" or triode system in which the substrate is self-biased by a supplementary r.f. generator not used to create the plasma.

(2) Tentative of reactor classification. We propose to classify the various plasma etchers according to the ratio ϕ_o/ϕ_i of the flux of neutral active species reaching the substrate relative to the ion flux impinging on it. It is obvious that the ϕ_o/ϕ_i ratio largely determines the anisotropic properties of etching.

(i) isotropic etching reactors ($\phi_o/\phi_i >> 1$): flowing afterglow etchers, microwave tunnel and tabular reactions are the main examples.

(ii) mainly isotropic etching reactors ($\phi_o/\phi_i > 1$) : the diode reactor in the plasma mode represents the current example.

(iii) mainly anisotropic etching reactors ($\phi_o/\phi_i \lesssim 1$) : the anisotropy is obtained by an enhancement in the ion density and the ion energy. Such reactors are characterized by a high ratio j_i/p, where j_i is the ion current density and p the pressure (142). This high ratio can be obtained either at low pressure reactive ion etching (59) (96), magnetron (145) or at high pressure in conjuction with high power density (>> 1 W/cm²) and a small electrode gap (5-10 mm) (142).

Kinetic analysis of the plasma reactor. Some simplifications have been made in order to understand, in a qualitative way, how the different parameters and the chemical reactions of the etching process are linked (78) (134) (147)-(150).

Winters et al. (78) considered the plasma as a blackbox in which the generation rate of fluorine atoms is supposed to proceed mainly via electron impact dissociation of CF_4. Mogab (134) proposed a continuity equation for the F active species in which the following processes are taken into account : generation of active species in the plasma volume, diffusion, etching, pumping losses. A law for an ideal loading effect is derived from this equation, in good agreement with experimental results for the silicon etching in a CF_4-O_2 radial flow reactor. In a similar analysis Mauer et al. (149) (150) tried to describe the reactive ion etching of silicon. Their model assumes that the enhancement of the etch rate by ion bombardment is the result of sputtering of SiF_x species. Turban et al. (89) constructed a very simple backmix reactor model of CF_4 plasma etching of silicon. In this analysis the first step is to consider the balance equation for the CF_4 molecules :

$$Q_M/V + P_v = S + N_M/t_R \qquad [26]$$

where Q_M is the input flow rate of CF_4 (molecules/sec), V the reactor volume, P_v represents an additional source of CF_4 (for example the reformation reaction $F + CF_3$), N_M is the concentration of CF_4 (cm^{-3}) and t_R the residence time. The primary decomposition rate of CF_4 (S) to proceed mainly via electron impact dissociation. This equation balances the source terms of CF_4 with the loss terms(dissociation and pumping). The second step in the analysis is to consider fluorine atoms. The generation rate of F atoms is supposed to be equal to S. Three loss terms are accounted for:

(i) the surface loss rate P_s, which is composed of silicon etching and the heterogeneous recombination of F atoms.

$$P_s \; (1/4)\, \varepsilon\, \bar{v}\, N_A\, A_{Si}/V + (1/4)\, \gamma\, \bar{v}\, N_A\, A_w/V \qquad [27]$$

where ε is the reaction probability of F on silicon (10^{-2} to 10^{-3}) for isotropic etching (115) (118) γ is the heterogeneous recombination coefficient of F atoms (109), $\bar{v}$ the mean random velocity of F atoms, N_A the concentration of fluorine, A_{Si} the silicon area to be etched and A_w the wall area of the reactor.

(ii) the volume loss rate P_v

(iii) the pumping loss rate.

This two fluid model provides a fairly good description of the experimental results obtained in the silicon etching with a CF_4-He plasma (89).

A similar multiple-etchant model proposed by Flamm et al. (149) gives a good representation of the loading effect observed for silicon etching in ClF_3 plasmas. Recent optical measurements of F density in CF_4-O_2 plasmas during the silicon etching exhibit trends which are well described by a kinetic analysis based on the continuity equation for F atoms (146).

Two recent detailed models have been published (90) (152) in which all the rates of the different chemical reactions involved in the CF_4 or $C_nF_m-O_2$ plasmas are considered. These emphasize how difficult it is to know reasonable values of the numerous reactions. In particular the work of Edelson and Flamm points out the lack of data for sticking coefficients and wall reaction efficiency, even in the simplest system , silicon etching in a CF_4 plasma. Much research effort will be needed in the experimental determination of these values for volume and wall reactions before one is able to obtain a quantitative description of the plasma etching process.

CONCLUSION

We have reviewed the basic mechanisms of amorphous silicon deposition from silane plasmas and silicon plasma etching with fluorinated plasmas. Recent progress in the diagnostics of these reactive discharges, both by mass spectrometry and optical spectroscopy, allow definition of the main hemogeneous and heterogeneous reactions: electron impact processes, ion-molecule reactions, radical reactions, deposition, spontaneous and ion-induced etching. There is still a long way to go before one will be able to have a complete quantitative approach of these phenomena.

Acknowledgement. I wish to thank the Scientific Committee of the 1983 I.U.P.A.C. Symposium on Plasma Chemistry for this invitation, and particularly Dr. Dan Flamm for his cordial encouragement in preparing this plenary lecture. I should like to express my gratitude to my colleagues and co-workers Dr Y. Catherine, Pr B. Grolleau, MM. J. Pasquereau, M. Rapeaux, P. Launay and A. Picard.

I also gratefully acknowledge the help of Dr. d'Agostino, Drs. Flamm, Haller, Perrin, Winters and Zarowin in providing preprints of their papers before publication.

REFERENCES

1. G. Turban, Thèse d'Etat, Université de Nantes, France (1981). University MicrofilmsInternational n° 82-70.021, 249 p.
2. I. Haller, J. Vac. Sci. Techn. A, (1983), in press.
3. P. Potzinger and F.W. Lampe, J. Phys. Chem. 73, 3912 (1969).
4. L.S. Polak and D.I. Slovetsky, Int. J. Radiat. Phys. Chem. 8, 257 (1976).
5. H.F. Winters, J. Chem. Phys. 63, 3462 (1975).
6. J. Perrin, J.P.M. Schmitt, G. de Rosny, B. Drevillon, J. Huc and A. Lloret, Chem. Phys. 73, 383 (1982).
7. Y. Harada, J.N. Murrel and H.H. Sheena, Chem. Phys. Letters, 1, 595 (1968).
8. G. Turban, Y. Catherine and B. Grolleau, Plasma Chem. Plasma Process. 2, 61 (1982).
9. C.A. De Joseph, Jr, A. Garscadden and D.R. Pond, Proceed. Laser's 82, New Orleans (1982).
10. J.F. O'Keefe and F.W. Lampe, Appl. Phys. Lett. 42, 217 (1983).
11. G. Turban, Y. Catherine and B. Grolleau, Thin Solid Films 77, 287 (1981).
12. G.C.A. Perkins, E.R. Austin and F.W. Lampe, J. Am. Chem. Soc. 101, 1109 (1979).
13. J. Perrin and J.P.M. Schmitt, Chem. Phys. 67, 167 (1982).
14. J. Perrin and J. Aarts, to be published (1983).
15. G. Turban, Y. Catherine and B. Grolleau, Thin Solid Films 60, 147 (1979).
16. G. Nolet, J. Electrochem. Soc. 122, 1030 (1975).
17. J.J. Wagner and S. Veprek, Plasma Chem. Plasma Process. 2, 95 (1982).
18. F.J. Kampas, J. Appl. Phys. 54, 2276 (1983).
19. H.A. Dewhurst and G.D. Cooper, J. Amer. Chem. Soc. 82, 4220 (1960).
20. G. Turban, Y. Catherine and B. Grolleau, Proc. of 4th Int. Symp. on Plasma Chemistry, Zurich , Vol. 1, 164 (1979).
21. G. Turban, Y. Catherine and B. Grolleau, Thin Solid Films, 67, 309 (1980).
22. J. Perrin and E. Delafosse, J. Phys. D : Appl. Phys. 13, 759 (1980).
23. F.J. Kampas and R.W. Griffith, Solar Cells. 2, 385 (1980).
24. F.J. Kampas and R.W. Griffith, J. Appl. Phys. 52, 1285 (1981).
25. M. Hirose, Amorphous Semiconductor, Edit. Y. Hamakawa (1982), p. 34.
26. A. Matsuda and K. Tanaka, Thin Solid Films. 92, 171 (1982).
27. T.Y. Yu, T.M.H. Cheng, V. Kemptner and F.W. Lampe, J. Phys. Chem. 76, 3321 (1972).
28. J.M.S. Henis, G.W. Stewart, M.K. Tripodi and P.P. Gaspar, J. Chem. Phys. 57, 389 (1972).
29. I. Haller, Appl. Phys. Lett. 37, 282 (1980).
30. B. Drevillon, J. Huc, A. Lloret, J. Perrin, and J.P.M. Schmitt, Appl. Phys. Lett. 37, 646 (1980).
31. H.A. Weakliem, Proc. 13 th A.I.A.A. Fluid and Plasma Dynamics Conf., July 1980, Snowmass, Colorado.
32. H.A. Weakliem, Proc. 3rd Symp. Plasma Processing, E.C.S. Denver, Oct. 1981, p. 14.
33. Y. Catherine, G. Turban and B. Grolleau, Thin Solid Films, 76, 23 (1981).
34. Y. Catherine, G. Turban and B. Grolleau, Plasma Chem. Plasma Process. 2, 81 (1982).
35. B. Drevillon, J. Huc, A. Lloret, J. Perrin, G. de Rosny and J.P.M. Schmitt, Proc. of 5th Int. Symp. on Plasma Chemistry, Edinburgh, Vol. 2, 634 (1981).
36. P. Kocian, J.M. Mayor and S. Bourquard, Proc. of 4th Int. Symp. on Plasma Chemistry, Zurich, Vol. 2, 663 (1979).
37. S. Bourquard, J.M. Mayor and P. Kocian, Journal de Phys. (Paris), 40, C7 – 385 (1979).
38. G. de Rosny, E.R. Mosburg, Jr, J.R. Abelson, G. Devaud and R.C. Kerns, J. Appl. Phys. 54, 2272 (1983).
39. J.C. Knights, J.P.M. Schmitt, J. Perrin and G. Guelachvili, J. Chem. Phys. 76, 3414 (1982).
40. N. Hata, A. Matsuda, K. Tanaka, K. Kajiyama, N. Moro and K. Sajiki, Japan. J. Appl. Phys. 22 , L 1 (1983).
41. G. Turban, Y. Catherine and B. Grolleau, Proc. of 5th Int. Symp. on Plasma Chemistry, Edinburgh, Vol. 2, 628 (1981).
42. A. Gallagher and J. Scott, Final Report S.E.R.I., Colorado (1981), unpublished.
43. J.C. Knights and G. Lucovsky, C.R.C. Crit. Rev. Solid State 9, 211 (1980).
44. H. Fritzche, Solar Energy Materials, 3, 447 (1980).
45. G. Turban and Y. Catherine, Thin Solid Films 48, 57 (1978).
46. I. Chen, Thin Solid Films 101, 41 (1983).
47. R.A. Street, J.C. Knights, D.K. Biegelsen, Phys. Rev. B18, 1880 (1978).
48. Y. Catherine, A. Zamouche, J. Bullot and M. Gauthier, Thin Solid Films, C (1983) in press.
49. B. Drevillon, J. Perrin, J.M. Sieffert, J. Hc, A. Lloret, G. de Rosny and J.P.M. Schmitt, Appl. Phys. Lett. to be published.
50. B.S. Meyerson, B.A. Scott and D.J. Wolford, J. Appl. Phys. 54, 1461 (1983).
51. J.C. Kinghts, J. Non-crystal. Solids, 35-36, 159 (1980).
52. B.A. Scott, M.H. Brodsky, D.C. Green, P.B. Kirby, R.M. Plecenik and E.E. Simonyi, Appl. Phys. Lett. 37, 725 (1980).
53. F.J. Kampas, J. Appl. Phys. 53, 6408 (1982).
54. S. Veprek, Pure Appl. Chem. 54, 1197 (1982).
55. A.P. Webb and S. Veprek, Chem. Phys. Lett. 62, 173 (1979).
56. T. Hamasaki, H. Kurata, M. Hirose and Y. Osaka, Appl. Phys. Lett. 37, 1084 (1981).
57. S. Veprek, Z. Iqbal, H.R. Oswald, F.A. Sarott and J.J. Wagner, Journal de Phys. (Paris), 42 , C4 - 251 (1981).
58. A.R. Reinberg, in VLSI Electronics : microstructure science, Vol. 2, N.G. Einspruch (Edit), Academic Press (1981).

59. D.J. Elliott, Integrated Circuit Fabrication Technology, Mac Graw Hill (1982).
60. C.M. Melliar-Smith and C.J. Mogab, in Thin Film Processes, J.L. Vossen and W. Kern (Edit.), Academic Press (1978).
61. J.W. Coburn and H.F. Winters, J. Vac. Sci. Technol. 16, 391 (1979).
62. D.L. Flamm, Solid State Technol. 22, 109 (1979).
63. E. Kay, J.W. Coburn and A. Dilks, Plasma Chemistry III, Topics in Current Chemistry n° 94, 1 (1980).
64. H.F. Winters, Plasma Chemistry III, Topics in Current Chemistry, n° 94, 69 (1980).
65. D.L. Flamm and V.M. Donnelly, Plasma Chem. Plasma Process 1, 317 (1981).
66. V.M. Donnelly and D.L. Flamm, Solid State Technol. 24, 161 (1981).
67. R.H. Bruce, Solid State Technol. 24, 64 (1981).
68. J.W. Coburn, Plasma Chem. Plasma Process 2, 1 (1982).
69. D.W. Hess, Plasma Chem. Plasma Process. 2 141 (1982).
70. D.L. Flamm, V.M. Donnelly and D.E. Ibbotson, J. Vac. Sci. Technol. B1, 23 (1983).
71. D.L. Flamm, Spring Meeting of Electrochem. Soc., San Francisco (May 1983), abstract n° 350.
72. P. Laporte, L. Peccoud and M. Chevalier, Microcircuit Engineering Conf., Lausanne (1981).
73. T.M. Mayer and R.A. Barker, J. Vac. Sci. Technol. 21, 757 (1982).
74. P.W. Harland and J.L. Franklin, J. Chem. Phys. 61, 1621 (1974).
75. L.G. Christophorou, Environment. Health. Persp. 36, 3 (1980).
76. S.M. Spyrou, I. Sauers and L.G. Christophorou, Proc. of Conf. on Gas Discharges, London (1982), p. 339.
77. H.U. Scheunemann, M. Heni, E. Illenberger and H. Baumgartel, Ber. Bunsenges. Phys. Chem. 86, 321 (1982).
78. H.F. Winters, J.W. Coburn and E. Kay, J. Appl. Phys. 48, 4973 (1977).
79. H.F. Winters and M. Inokuti, Phys. Rev. A 25, 1420 (1982).
80. R. d'Agostino, F. Cramarossa, S. de Benedictis and g. Ferraro, J. Appl. Phys. 52, 1259 (1981).
81. R. d'Agostino, F. Cramarossa, S. de Benedictis, Plasma Chem. Plasma Process. 2, 213 (1982).
82. R. d'Agostino, F. Cramarossa, V. Colaprico and R. d'Ettole, J. Appl. Phys. 54, 1284 (1983).
83. J.W. Coburn and M. Chen, J. Appl. Phys. 51, 3134 (1980).
84. J.W. Coburn and M. Chen, J. Vac. Sci. Technol. 18, 353 (1981).
85. R. d'Agostino, V. Colaprico and F. Cramarossa 1, 365 (1981).
86. G. Smolinsky and D.L. Flamm, J. Appl. Phys. 50, 4982 (1979).
87. E.A. Truesdale and G. Smolinsky, J. Appl. Phys. 50, 6595 (1979).
88. E.A. Truesdale, G. Smolinsky and T.M. Mayer 51, 2909 (1980).
89. G. Turban, J. Pasquereau, M. Rapeaux, Y. Catherine and B. Grolleau, Proceed. 3rd Symp. Plasma Process., E.C.S., Denver (1981), p. 45.
90. M.J. Kushner, J. Appl. Phys. 53, 2923 (1982).
91. M.J. Kushner, J. Appl. Phys. 53, 2939 (1982).
92. P.J. Hargis jr and M.J. Kushner, Appl. Phys. Lett. 40, 779 (1982).
93. M.J. Vasile and G. Smolinsky, J. Phys. Chem. 81, 2605 (1977).
94. G. Turban, P. Launay and B. Grolleau unpublished results (1983).
95. G. Turban, J. Pasquereau, M. Rapeaux, Y. Catherine and B. Grolleau, unpublished results (1981).
96. Ch. Steinbrüchel, J. Electrochem. Soc. 130, 648 (1983).
97. M.J.K. Pabst, H.S. Tan and J.L. Franklin, Int. J. Mass Spectrom. Ion Phys. 20, 191 (1976).
98. J.W. Coburn and E. Kay, Proc. 7th Intern. Vac. Congr. and 3rd Conf. Solid Surfaces, Vienna, (1977), p. 1257.
99. C.I.M. Beenakker, R.P.J. Van de Poll, and J. Dieleman, Proceed. 3rd Symp. Plasma Process., E.C.S., Denver (1981) p. 401.
100. R.A.H. Heinecke, Solid State Electron 19, 1039 (1976).
101. L.M. Ephrath, J. Electrochem. Soc. 124, 284 (1977).
102. H.W. Lehmann and R. Widmer, J. Vac. Sci. Technol. 15, 319 (1978).
103. J.W. Coburn, J. Appl. Phys. 50, 5210 (1979).
104. J.W. Coburn and E. Kay, I.B.M. J. Res. Develop. 23, 33 (1979).
105. D.L. Flamm, J. Appl. Phys. 51, 5692 (1980).
106. E. Kay and A. Dilks, ACS Symp. Ser. 108, Plasma Polymerisation, (M. Shen, A.T. Bell Ed.), (1979) p. 195.
107. M.M. Millard and E. Kay, J. Electrochem. Soc. 129, 160 (1982).
108. D.L. Flamm, Plasma Chem. Plasma Process. 1, 37 (1981).
109. C.J. Mogab, A.C. Adams and D.L. Flamm, J. Appl. Phys. 49, 3796 (1978).
110. Y. Horiike and M. Shibagaki, Jap. J. Appl. Phys. 15, 13 (1976).
111. F.H.M. Sanders, J.H.J. van Dommelen, J.A.M. Sanders, C.I.M. Beenaker and J. Dieleman, Proceed. Plasma Process. E.C.S., Saint-Louis (1980), p. 155.
112. C.I.M. Beenaker, J.H.J. van Dommelen and R.P.J. van de Poll, J. Appl. Phys. 52, 480 (1981).
113. K.R. Ryan and I.C. Plumb, J. Phys. Chem. 86, 4678 (1982).
114. R. d'Agostino and D.L. Flamm, J. Appl. Phys. 52, 162 (1981).
115. D.L. Flamm, V.M. Donnelly, and J.A. Mucha, J. Appl. Phys. 52, 3633 (1981).
116. G. Turban and M. Rapeaux, Spring Meeting of Electrochem. Soc., San Francisco, (May 1983), abstract n° 177.
117. G. Turban and A. Picard, unpublished results (1983).
118. M.J. Vasile and F.A. Stevie, J. Appl. Phys. 53, 3799 (1982).
119. V.M. Donnelly and D.L. Flamm, J. Appl. Phys., 51, 5273 (1980).
120. J.A. Mucha, D.L. Flamm, V.M. Donnelly and L.M. Webb, J. Phys. Chem. 84, 3529 (1981).

121. C.I.M. Beenaker, J.H.J. van Dommelen and J. Dieleman, 157th Meeting of Electrochem. Soc., Saint-Louis (1980), Abstract n° 126.
122. H.F. Winters and J.W. Coburn, Appl. Phys. Lett. 34, 70 (1979).
123. Y.Y. Tu, T.J. Chuang and H.F. Winters, Phys. Rev. B 23, 823 (1981).
124. H.F. Winters and F.A. Stevie, J. Appl. Phys. 53, 3799 (1982).
125. H.F. Winters, J.W. Coburn and T.J. Chuang, to be published (1983).
126. D.L. Flamm, D.E. Ibbotson, J.A. Mucha and V.M. Donnelly, Solid State Technol., April (1983).
127. D.E. Ibbotson, D.L. Flamm, J.A. Mucha and V.M. Donnelly, submitted to Appl. Phys. Lett. (1983).
128. U. Gerlach-Meyer, J.W. Coburn and E. Kay, Surf. Sci. 103, 177 (1981).
129. E.A. Knabbe, J.W. Coburn and E. Kay, Surf. Sci. 123, 427 (1982).
130. T.J. Chuang, J. Appl. Phys. 51, 2614 (1980).
131. C.J. Mogab and H.J. Levinstein, J. Vac. Sci. Technol., 17, 721 (1980).
132. D.L. Flamm, C.J. Mogab and E.R. Sklaver, J. Appl. Phys. 50, 6211 (1979).
133. S. Matsuo, J. Vac. Sci. Technol. 17, 587 (1980).
134. C.J. Mogab, J. Electrochem. Soc. 124, 1262 (1977).
135. J. Taillet, Proc. 7th Int. Symp. Plasma Chemistry, Zurich (1979), Vol.1 p. 113.
136. R.H. Bruce, J. Appl. Phys. 52, 7064 (1981).
137. B.N. Chapman and V.J. Minkiewicz, J. Vac. Sci. Technol. 15, 329 (1978).
138. B.N. Chapman and T.A. Hansen, J. Appl. Phys. 51, 3608 (1980).
139. B.N. Chapman, Glow discharge processes, Wiley (1980).
140. V.M. Donnelly, D.L. Flamm, C.W. Tu and D.E. Ibbotson, J. Electrochem. Soc. 129, 2533 (1982).
141. J.W. Coburn and E. Kay, J. Appl. Phys. 43, 4965 (1972).
142. A.R. Reinberg, J. Dalle-Ave, G. Steinberg and R. Bruce, Proc. 3rd Symp. Plasma Process. ; E.C.S. Denver (1981) p. 198.
143. C.B. Zarowin and R.S. Horwath, J. Electrochem. Soc. 129, 2541 (1982).
144. R.H. Bruce and A.R. Reinberg, J. Electrochem. Soc. 129, 393 (1982).
145. H. Okano and Y. Horiike, Proceed 3rd Symp. Plasma Process, E.C.S., Denver (1981), p. 206.
146. H. Kawata, T. Shibano, K. Murata and K. Nagami, J. Appl. Phys. 54, 2720 (1983).
147. J.W. Coburn and E. Kay, J. Macromol. Sci. Chem., A10, 483 (1976).
148. J.F. Battey, J. Electrochem. Soc. 124, 437 (1977).
149. J.L. Mauer, J.S. Logan, L.B. Zielinski and G.C. Schwartz, J. Vac. Sci. Technol. 15, 1734 (1978).
150. J.L. Mauer, J.S. Logan, J. Vac. Sci. Technol. 16, 404 (1979).
151. D.L. Flamm, D.N.K. Wang and D. Maydan, J. Electrochem. Soc. 129, 2755 (1982).
152. D. Edelson and D.L. Flamm, J. Appl. Phys., to appear (1983).
153. J.G. Calvert and J.N. Pitts jr, Photochemistry, Wiley (1966).
154. J. Heicklen, Advances in Photochemistry, Interscience, New York (1969) Vol.7, p. 58.
155. J.A. Beran and L. Kevan, J. Phys. Chem. 73, 3866 (1969).
156. D.L. Hobrock and R.W. Kiser, J. Phys. Chem. 68, 575 (1964).
157. A. Chutjian, Phys. Rev. Lett. 46, 1511 (1981).
158. L.E. Kline, D.K. Davies, C.L. Chen and P.J. Chantry, J. Appl. Phys. 50, 6789 (1979).
159. C.L. Chen and P.J. Chantry, J. Chem. Phys. 71, 3897 (1979).
160. V.H. Dibeler and F.L. Mohler, J. Res. Nat. Bur. Stand. 40, 25 (1948).
161. T. Stanski and B. Adamczyk, Int. J. Mass. Spectrom. Ion Phys. 46, 31 (1983).
162. G.J. Verhaart, H.A. Van Sprang and H.H. Brongersma, Chem. Phys. 51, 389 (1980).
163. H.J. Tiller, D. Berg and R. Mohr, Plasma Process. Plasma Chem. 1, 247 (1981).
164. K. Tachibana, H. Tadokoro, H. Harima and Y. Urano, J. Phys. D : Appl. Phys. 15, 177 (1982).
165. J.P.M. Schmitt, Gressie, Krishan, J. Perrin, G. de Rosny, submitted to Chem. Phys. (1983).
166. M. Venugopalan and S. Veprek, Topics in Current Chemistry n° 107, Plasma Chemistry IV, Springer-Verlag (1983).
167. C.M. Horwitz, J. Vac. Sci. Technol. A1, 60 (1983).